Priority Communication

Identification of nitrites/HONO as primary products of NO oxidation over Fe-ZSM-5 and their role in the Standard SCR mechanism: A chemical trapping study

Maria Pia Ruggeri, Tommaso Selleri, Massimo Colombo, Isabella Nova, Enrico Tronconi *

Dipartimento di Energia, Laboratorio di Catalisi e Processi Catalitici, Politecnico di Milano, Piazza Leonardo da Vinci 32, I-20133 Milano, Italy

Article history:
Received 11 October 2013
Revised 19 November 2013
Accepted 30 November 2013
Available online 3 January 2014

1. Introduction

Compliance with current NO_x emission limits from Diesel vehicles requires the application of exhaust gas aftertreatment technologies, such as Lean NO_x Traps (LNT) or NH_3/Urea-Selective Catalytic Reduction (NH_3/Urea-SCR). In NH_3-SCR catalytic converters, excellent deNO_x performances can be attained on the account of the Standard SCR reaction ($NO + O_2 + NH_3$) and especially of the Fast SCR reaction ($NO + NO_2 + NH_3$) [1]. In recent years, several research efforts [1–9] were aimed at the study of the SCR catalytic mechanism and at the identification of related intermediate species both in the gas phase and on the catalyst surface. A number of techniques have been employed, including Transient Response Methods for the analysis of gaseous species evolution and *in situ* IR spectroscopy for the investigation of surface species. Due to its efficiency in reducing NO_x at low temperatures, the attention has been mostly focused on the Fast SCR reaction. A general agreement on the Fast SCR mechanism has been achieved, identifying the reduction of surface nitrates to nitrites by NO as the rate determining step at low temperature [5,10]. The Standard SCR chemistry, however, is still subject of debate. In particular, several publications have recently investigated the relationship between NO oxidation to NO_2 and Standard SCR on Fe- and Cu-promoted zeolites to clarify the similarities and the discrepancies in the mechanisms of these two reactions [11–15]. We have recently reported multiple experimental evidence to show that NO oxidation to gaseous NO_2 cannot be the rate determining step of the Standard SCR reaction [16]. An alternative mechanistic hypothesis [16] relies on nitrite ad-species, NO_2^-, in equilibrium with gaseous nitrous acid, HONO, acting as common intermediates in the mechanisms of both the NO oxidation [17] and the $NO + NH_3$ Standard SCR reactions [18]. Due to their instability and high reactivity, however, NO_2^- and HONO can hardly be detected in reacting conditions. Moreover, IR spectroscopic techniques cannot be used to identify nitrite ad-species on metal-promoted zeolite catalysts, since their characteristic bands, e.g. at 1260 cm^{-1}, fall in the absorbance region of the zeolite framework (wavenumbers <1300 cm^{-1}) [10,19]. Indirect evidence of the relevance of nitrite-like species in the SCR mechanism comes from the *in situ* FTIR detection of NO^+ species (nitrosonium ions) both on Fe- and on Cu-zeolite catalysts [10,20]: nitrosonium ions are in fact characterized by the same N oxidation state of nitrites (+3), and are likely in equilibrium with nitrites [10,20]. Nevertheless, a direct proof of the involvement of nitrites in both the NO oxidation and the Standard SCR mechanisms is still lacking to our knowledge.

We present herein a novel approach to the identification of NO_x reacting intermediates in SCR catalysis. To this scope, two different materials, namely a Fe-ZSM-5 commercial catalyst, playing the role of active phase, and in-house prepared BaO/Al_2O_3, acting as

* Corresponding author. Fax: +39 02 2399 3318.
E-mail address: enrico.tronconi@polimi.it (E. Tronconi).

chemical trap, have been combined to activate a synergic interaction of their functionalities. Specifically, BaO/Al_2O_3 has been chosen for its capability to store stable nitrites and nitrates, as well known from the LNT literature [21]. A mechanical mixture of Fe-ZSM-5 and BaO/Al_2O_3 powders was prepared and loaded in a flow micro reactor, and simple experiments, focused on low temperature, 120 °C, involving the transient feed of both NO and O_2 were performed. The goal was to trap on the BaO phase the intermediates possibly formed by interaction of NO and O_2 with the Fe-ZSM-5 catalyst. Information on the chemical nature of trapped ad-species was then gained in the first place by studying their thermal decomposition via Temperature Programmed Desorption (TPD). More chemical evidence was collected by probing the reactivity of the trapped intermediates with NH_3. Finally, e*x situ* IR spectroscopy was also applied to conclusively identify the intermediates captured by the BaO component of the Fe-ZSM-5 + BaO/Al_2O_3 mixture.

2. Experimental

A mechanical mixture of Fe-ZSM-5 (22 mg) and of BaO/Al_2O_3 (44 mg) powders was used in the present study. The relative amounts of the two components ensured a large excess of potential Ba storage sites in comparison with the Fe sites. The Fe-promoted zeolite was a commercial (Zeolyst) catalyst with a Si/Al ratio of 12 and 1% w/w Fe content. The original zeolite powder was dried at 120 °C for 4 h and sieved to 120–140 mesh (average particle size = 115 μm). The BaO/Al_2O_3 component (Ba content = 16% w/w) was prepared in-house by the incipient wetness impregnation method, using aqueous solutions of $Ba(CH_3COO)_2$ (Strem Chemical, 99%) to impregnate the γ-alumina support calcined at 700 °C (Versal 250 from La Roche Chemicals: surface area = 200 m^2/g and pore volume = 1.2 cm/g). After impregnation, the powder was dried at 80 °C overnight, calcined at 500 °C for 5 h, and sieved to 140–200 mesh (average particle size = 90 μm). The two powdered phases were mixed and diluted up to 160 mg with cordierite (120–140 mesh) before being loaded in a quartz microreactor (i.d. ≈6 mm) where the bed was suspended by means of quartz wool. This resulted in a packed bed approximately 1 cm deep. To enhance the gas mixing, a bed of quartz grains was placed upstream of the catalyst powder. The reactor was inserted in a vertical electric furnace and its temperature was controlled by a K-type thermocouple in contact with the top of the catalytic bed, which was located in the isothermal zone of the furnace. Helium was used as balance gas in all the micro-reactor runs. Gases were dosed using mass flow controllers (Brooks Instruments), while water vapor was added to the feed stream by means of a saturator operated at controlled temperature. A blank transient without catalyst powder confirmed a step change NO inlet profile. The catalyst bed was initially conditioned flowing 10% v/v of O_2 and H_2O for 6 h at 600 °C. Prior to each experiment, the catalyst was pretreated feeding 8% v/v O_2 and 10% v/v H_2O for 1 h at 550 °C. In a typical adsorption run 500 ppm of NO and 8% v/v O_2, in a total volumetric flow of 120 cm^3/min (STP), were fed to the reactor at 120 °C. The pressure drop was of the order of 0.1 bar. The temporal evolution of the species at reactor outlet was monitored by a quadrupole mass spectrometer (Balzers QMS 200) and a UV analyzer (ABB LIMAS 11 HW) arranged in a parallel configuration. The setup enabled the simultaneous analysis of NO, NO_2, NH_3 (by UV analyzer and by MS), N_2, N_2O and H_2O (by MS) [3,22]. In some runs, the isothermal adsorption phase was followed by a TPD phase up to 550 °C (15 °C/min). In other experiments, the NO + O_2 feed was replaced by a feed with 500 ppm NH_3, still at 120 °C: in this case NO was step changed to NH_3, whereas O_2 was replaced by He to keep the volumetric flow unchanged.

Ex situ FTIR measurements were performed with a Thermo Nicolet Nexus 870 FTIR instrument, after unloading the catalyst bed from the quartz reactor after NO + O_2 adsorption at 120 °C. The mechanical mixture for these experiments included 30 mg of Fe-ZSM-5 and 60 mg of BaO/Al_2O_3 but no cordierite for powders dilution. Moreover, the particle size of the two phases was inverted (Fe-ZSM-5 = 90 μm, BaO/Al_2O_3 = 115 μm), in order to facilitate their separation by sieving. Pelletized samples for the IR analysis were prepared by dilution with KBr, loaded in a sample holder and placed in the sample compartment of the FTIR instrument. A background spectrum was collected prior to the analysis. All the IR spectra were recorded with 64 scans/run and a 2 cm^{-1} resolution. Reference spectra of the clean Fe-ZSM-5 and of the clean BaO/Al_2O_3 powders, after the same pre-conditioning procedure already discussed, were used for subtraction and display of the IR spectra in the absorbance mode.

3. Results and discussion

3.1. Transient reaction analysis: NO + O_2 adsorption and TPD

Fig. 1 shows the two stages of a micro-reactor experiment in which NO and O_2 were co-fed at 120 °C to the mechanical mixture prepared from the Fe-ZSM-5, BaO/Al_2O_3 and cordierite powders. In Fig. 1A (isothermal adsorption phase), the NO outlet concentration trace shows a delay of around 25 s with respect to the NO inlet profile. Moreover, the NO outlet concentration dynamics are very slow, approaching steady state after over 2000 s. Simultaneous NO_2 evolution is observed: NO_2 exhibits a dead time of over 200 s, then its concentration slowly increases up to about 30 ppm.

Once NO and NO_2 reached steady state, NO and O_2 were shut off and the temperature was ramped up to 550 °C. The TPD results in Fig. 1B show simultaneous desorption of NO and NO_2 in approximately equimolar amounts (confirmed by both the UV analyzer and the MS), with a maximum at 200 °C. Equimolar NO and NO_2 desorption continued up to 370 °C, at which temperature the NO release began to exceed NO_2 desorption, likely due to the onset of NO_2 decomposition to NO + O_2 on Fe sites. The integral of NO_x stored during the adsorption phase differed from the total NO_x desorbed during the TPD by less than 10%. The moles of desorbed NO_x correspond to about 13% of the overall number of Fe + Ba sites: similar occupations of Ba sites are reported in the LNT literature [23].

While NO oxidation is known to be negligible over BaO/Al_2O_3, Fe-zeolite catalysts exhibit a good activity in NO oxidation already at 150 °C in the absence of H_2O [24]. A red-ox mechanism for NO oxidation to NO_2 has been proposed recently for both Cu- and Fe-zeolite catalysts [16]. In particular, for Fe-zeolites, assuming the active centers to be monomeric hydroxylated ferric sites [25] and starting from the catalyst in an oxidized state, the mechanism at low temperature can be formulated as follows:

$$Fe^{3+}OH + NO \leftrightarrow Fe^{2+} + HONO \quad (R.1)$$

$$HONO + Fe^{3+}OH \leftrightarrow Fe^{3+}ONO + H_2O \quad (R.2)$$

$$Fe^{3+}ONO \rightarrow Fe^{2+} + NO_2 \quad \textbf{rate determining} \quad (R.3)$$

$$2Fe^{2+} + \frac{1}{2}O_2 + H_2O \rightarrow 2Fe^{3+}OH \quad (R.4)$$

All the steps included in the red-ox mechanism above were independently proposed in previous FTIR literature studies [4,26,27] and are jointly discussed in [16]. According to R.1–R.4, NO oxidation to NO_2 proceeds via a two-step (R.1 and R.2) formation of ferric nitrites, which are in equilibrium with HONO in the gas phase. This

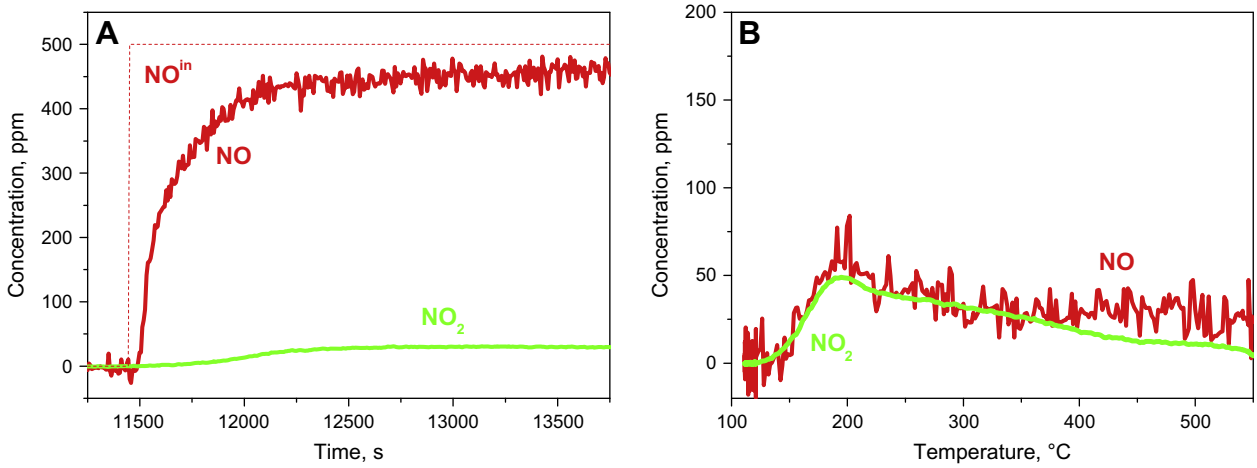

Fig. 1. (A) NO + O_2 adsorption at 120 °C on the Fe-ZSM-5 + BaO/Al_2O_3 mechanical mixture. T = 120 °C; Q = 120 cm^3/min (STP); feed: H_2O = 0%; O_2 = 8%; NO = 500 ppm in He and (B) Subsequent TPD run: T = 120–550 °C; heating rate = 15 K/min; feed: H_2O = 0%; O_2 = 0% in He.

equilibrium (i.e. step R.2) explains the well known strong H_2O inhibition of NO oxidation [4,16], as an increased H_2O concentration would shift the equilibrium to the left reducing the nitrites surface concentration and thus the rate of NO_2 formation, R.3. The nitrites/HONO equilibrium is also quite relevant to rationalize the results in Fig. 1A. Since the NO oxidation activity over BaO/Al_2O_3 is negligible [28], and NO + O_2 adsorption at 120 °C was found insignificant on Fe-ZSM-5 and very limited on BaO/Al_2O_3 (one order of magnitude less than on the physical mixture), the considerable storage observed when feeding NO + O_2 to the Fe-ZSM-5 + BaO/Al_2O_3 mechanical mixture reveals an interaction between the two system components via gas phase, which is nicely in line with the above proposed mechanism. In this case, in fact, gaseous HONO formed by NO oxidation over Fe sites in step R.1 can interact either with another oxidized Fe site or with BaO to form Fe-ONO or $Ba(NO_2)_2$ according to R.2 or to R.5, respectively:

$$BaO + 2HONO \leftrightarrow Ba(NO_2)_2 + H_2O \qquad (R.5)$$

Step R.5 would be thus responsible for the formation of stable nitrites on Ba. The equilibrium between Fe-nitrites and Ba-nitrites via gas-phase HONO also explains the peculiar dynamics apparent in Fig. 1A, wherein the NO_2 product takes so long to break through. In fact, during NO + O_2 adsorption, the less abundant Fe sites are busy at first with oxidizing NO to HONO (R.1), while the BaO phase becomes progressively saturated with stable nitrites (R.5). After BaO saturation is approached, HONO can eventually start forming less stable nitrites also on the Fe sites (R.2), which slowly decompose to gaseous NO_2, R.3 being the rate determining step of the overall NO to NO_2 process [16,17]. Notice that, since BaO is already occupied by the nitrites, NO_2 is unable to store so many nitrates as it would if BaO were free; also, NO_2 is apparently unable to convert the stored nitrites to nitrates at these conditions.

During the following TPD phase, Fig. 1B, also the more stable Ba-nitrites decompose via gaseous HONO according to steps R.5 reverse and R.6 [29]:

$$Ba(NO_2)_2 + H_2O \leftrightarrow BaO + 2HONO \qquad (R.5reverse)$$

$$2HONO \rightarrow NO + NO_2 + H_2O \qquad (R.6)$$

which well explains the desorption of NO and NO_2 in equimolar proportions noted in Fig. 1B. Notably, no net H_2O formation would be expected from the combination of R.5 reverse and R.6: on the contrary, some H_2O release was noted during the TPD, possibly due to H_2O desorption from the zeolite or to the interaction of HONO with the zeolite and/or with the Fe–OH sites.

It should be emphasized that the decomposition profiles obtained from the TPD following NO + O_2 adsorption, shown in Fig. 1B, are completely different from those recorded after NO_2 adsorption both on BaO/Al_2O_3 and on Fe-zeolites [30,31]: in the latter case, in fact, NO_2 gets stored in the form of nitrates, and essentially just NO_2 is desorbed during the subsequent TPD, along with O_2 and H_2O, in line with the thermal decomposition of nitrates [31]: some NO is observed only at high temperatures as a result of NO_2 decomposition. This provides additional evidence that NO_2 is not an intermediate in NO + O_2 reactions over Fe-zeolite catalysts.

3.2. Transient reaction analysis: NO + O_2 adsorption and surface reaction with NH_3

Fig. 2 shows the second stage of an isothermal transient run wherein the Fe-ZSM-5 + BaO/Al_2O_3 mechanical mixture was first exposed to NO + O_2 at 120 °C, like in Fig. 1A, followed by replacing NO + O_2 with NH_3 (500 ppm) in the feed stream: in addition to the expected NH_3 dead time due to ammonia adsorption onto the Fe-zeolite, a significant N_2 evolution was observed. This is extra evidence in favor of nitrites/HONO being formed and trapped during the NO + O_2 adsorption phase, as they are well known to react readily with NH_3 forming dinitrogen at T > 100 °C via decomposi-

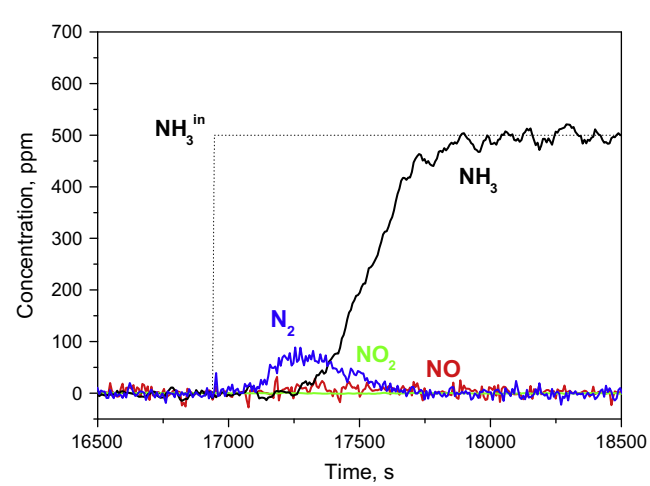

Fig. 2. Pulse of NH_3 after NO + O_2 adsorption on the Fe-ZSM-5 + BaO/Al_2O_3 mechanical mixture. T = 120 °C; Q = 120 cm^3/min (STP); feed: H_2O = 0%; O_2 = 0%; NH_3 = 500 ppm in He.

tion of unstable ammonium nitrite [6,9,10,32]. On a molar basis, the nitrogen release in Fig. 2 corresponds to about 23% of the total NO_x desorbed in Fig. 1B (9.2 μmol). Further N_2 evolution was observed upon increasing the temperature (not shown): the overall measured N_2 formation (9.4 μmol) was eventually well in line with the total NO_x evolution.

One mechanistic scheme in line with the data in Fig. 2 is as follows:

$$NH_3 + Z - OH \leftrightarrow Z - ONH_4 \quad (R.7)$$

$$HONO + Z - ONH_4 \rightarrow [NH_4NO_2] + Z - OH \rightarrow N_2 + 2H_2O + Z - OH \quad (R.8)$$

with Z–OH representing an acidic zeolite site, and HONO originating from the nitrites stored on Fe or BaO via steps R.2 and R.5 reverse. Evolution of H_2O was also detected by MS in parallel to the N_2 release, which is consistent with the proposed mechanism.

Notably, direct reactivity of NH_3 with nitrates to give N_2 is observed over Fe-zeolites only at much higher temperatures (T > 220–230 °C) [7,33] and can therefore be ruled out in our experiments at 120 °C. The results in Fig. 2 are obviously relevant for the elucidation of the Standard SCR mechanism.

3.3. Ex situ IR analysis

IR spectroscopy was used to conclusively confirm the formation of nitrites ad-species from NO + O_2. A NO + O_2 adsorption run at 120 °C was replicated over the Fe-ZSM-5 + BaO/Al_2O_3 mechanical mixture: in this case, at the end of the isothermal adsorption phase the powdered mixture was unloaded from the reactor. The two components of the mechanical mixture were then separated by sieving, taking advantage of the different particle sizes of the Fe-zeolite and BaO/Al_2O_3 powders, and IR spectra were recorded. On the Fe zeolite, no IR bands related to nitrates or nitrites could be detected, possibly due to the masking effect of the zeolite matrix. Indeed, no nitrates are expected to be present under NO + O_2 feed at 120 °C, since nitrates possibly formed on the Fe-zeolite would be reduced by the excess of NO in the gas phase [10]. On the other hand, the vibrations of nitrites would be masked by the bands associated with the zeolite framework (wavenumbers <1300 cm^{-1}) [19]. On the contrary, several bands were detected by *ex situ* IR analysis of the unloaded BaO/Al_2O_3 powder, as shown in Fig. 3. The most prominent feature is a broad band centered around 1100 cm^{-1}, assigned to ν_{N-O} modes of Ba-nitrites [34,35]. Moreover, the two partially overlapped peaks with maxima located at 1220 and 1270 cm^{-1} can be further assigned to nitrite ad-species: in particular, the 1220 cm^{-1} band to the ν_{asym} of NO_2

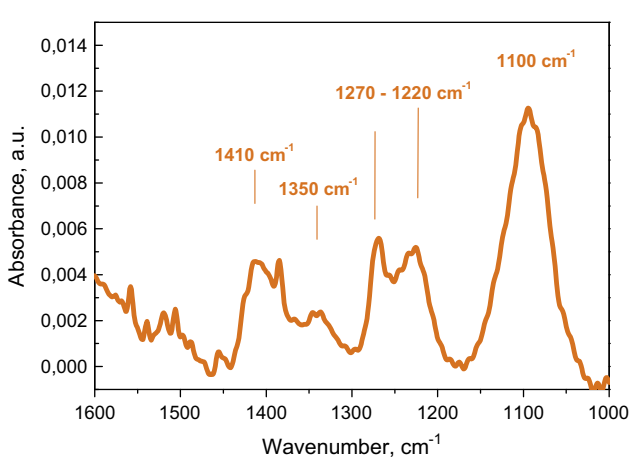

Fig. 3. NO + O_2 adsorption on the Fe-ZSM-5 + BaO/Al_2O_3 mechanical mixture at 120 °C: ex situ IR analysis of the BaO/Al_2O_3 component unloaded from the test reactor.

associated with ionic nitrites [21,28,34,36] and the 1270 cm^{-1} band to free NO_2^- nitrite ions [9,36–38]. The assignment of the band at 1270 cm^{-1} is indeed controversial: the same band has been attributed to either nitrite ions or to the ν_{asym} NO_2 of bidentate nitrates formed on γ-Al_2O_3 [28,39,40]. Both interpretations are suitable, although the assignment of the 1270 cm^{-1} band to nitrite ions is better in line with our observations: in fact, this band was not present in IR spectra collected with the same method at steady state after NO_2 adsorption on the BaO/Al_2O_3 powder, i.e. when only nitrates are expected to be stored on the catalyst surface [28,30,40]. The presence of the free nitrite ions is furthermore a proof of the equilibrium prevailing between adsorbed nitrites and gas-phase HONO, e.g. via steps R.2 and R.5.

The 1350 cm^{-1} band has been also observed [21] during the co-adsorption of NO and O_2 at 150 °C on BaO-Al_2O_3 and assigned to ν_{sym} of NO_2, belonging to chelating nitrites. Traces of nitrates are also apparent in Fig. 3: e.g. the bands at 1410 cm^{-1} can be assigned to $\nu_{NO3,sym}$ of ionic nitrates [28].

In summary, several nitrite ad-species have been thus detected on the BaO phase of the mechanical mixture. The IR analysis is therefore in full agreement with the proposed mechanisms and directly supports the identification of NO_2^- and HONO as intermediates of NO oxidation and Standard SCR reactions over Fe-ZSM-5, as never reported so far in the scientific literature on zeolite-based SCR catalysis.

4. Conclusions

Nitrites/HONO, often proposed as unstable reactive intermediates of the NO oxidation, Standard and Fast SCR reactions over metal-exchanged zeolites, had never been indisputably detected so far. Based on chemical trapping techniques, we present herein for the first time clear and multiple evidence of their formation during the oxidative activation of NO over a commercial Fe-ZSM-5 catalyst. The inclusion of BaO/Al_2O_3 in a physical mixture with Fe-ZSM-5 resulted in stabilizing nitrite ad-species formed over the Fe-sites after exposure to NO + O_2 at 120 °C and captured onto BaO via gas-phase equilibrium with HONO.

Identification of the nitrites trapped onto BaO is confirmed: (i) by their thermal decomposition to an equimolar mix of NO and NO_2 during TPD, (ii) by N_2 formation as a result of their reactivity with NH_3, and finally (iii) by *ex situ* IR analysis of the BaO powder after discharge of the mechanical mixture from the test reactor and separation of its components. The present data strongly suggest an equilibrium between surface nitrites (on both Fe-ZSM-5 and BaO phases) and gaseous HONO, which well explains the observed interactions between the two materials. On the other hand, our data rule out NO_2 as the primary product of the NO oxidative activation over Fe-ZSM-5: parallel experiments with NO_2 (not presented here) in fact demonstrate the formation of nitrates/HNO_3, instead of the nitrites/HONO herein observed when feeding NO + O_2.

Considering that nitrites/HONO decompose to NO_2 during NO oxidation, and react with NH_3 to give N_2, they seem therefore strong candidates as key intermediates for both reactions. The relevance of these findings for the mechanistic and kinetic description of the Standard SCR chemistry over Fe- and Cu-zeolite catalysts will be discussed in more details in a forthcoming extended paper.

References

[1] S. Brandenberger, O. Kröcher, A. Tissler, R. Althoff, Catal. Rev. 50 (2008) 492.
[2] C. Ciardelli, I. Nova, E. Tronconi, D. Chatterjee, B. Bandl-Konrad, Chem. Commun. (2004) 2718.
[3] I. Nova, C. Ciardelli, E. Tronconi, D. Chatterjee, B. Bandl-Konrad, Catal. Today 114 (2006) 3.
[4] Y.H. Yeom, J. Henao, M.J. Li, W.M.H. Sachtler, E. Weitz, J. Catal. 231 (2005) 181.

[5] A. Grossale, I. Nova, E. Tronconi, D. Chatterjee, M. Weibel, J. Catal. 256 (2008) 312.
[6] A. Savara, M.-J. Li, W.M.H. Sachtler, E. Weitz, Appl. Catal. B: Environ. 81 (2008) 251.
[7] A. Grossale, I. Nova, E. Tronconi, Catal. Lett. 130 (2009) 525.
[8] A. Grossale, I. Nova, E. Tronconi, J. Catal. 265 (2009) 141.
[9] A. Savara, W.M.H. Sachtler, E. Weitz, Appl. Catal. B: Environ. 90 (2009) 120.
[10] M.P. Ruggeri, A. Grossale, I. Nova, E. Tronconi, H. Jirglova, Z. Sobalik, Catal. Today 184 (2012) 107.
[11] J.R. Klovsky, P.B. Koradia, C.T. Lim, Ind. Eng. Chem. Prod. Res. Dev. 19 (1980) 218.
[12] R.Q. Long, R.T. Yang, J. Catal. 207 (2002) 224.
[13] H. Sjövall, R.J. Blint, L. Olsson, Appl. Catal. B: Environ. 92 (2009) 138.
[14] M. Iwasaki, K. Yamazaki, H. Shinjoh, Appl Catal A: Gen 366 (2009) 84.
[15] P.S. Metkar, M.P. Harold, V. Balakotaiah, Appl. Catal. B: Environ. 111–112 (2012) 67.
[16] M. Ruggeri, I. Nova, E. Tronconi, Top. Catal. 56 (2013) 109.
[17] G. Delahay, D. Valade, A. Guzmán-Vargas, B. Coq, Appl. Catal. B: Environ. 55 (2005) 149.
[18] Q. Sun, Z.-X. Gao, B. Wen, W.H. Sachtler, Catal. Lett. 78 (2002) 1.
[19] M. Rivallan, G. Ricchiardi, S. Bordiga, A. Zecchina, J. Catal. 264 (2009) 104.
[20] J.H. Kwak, J.H. Lee, S.D. Burton, A.S. Lipton, C.H.F. Peden, J. Szanyi, Angew. Chem. Int. Ed. 52 (2013) 9985.
[21] L. Lietti, M. Daturi, V. Blasin-Aubé, G. Ghiotti, F. Prinetto, P. Forzatti, ChemCatChem 4 (2012) 55.
[22] C. Ciardelli, I. Nova, E. Tronconi, M. Ascherfeld, W. Fabinski, Top. Catal. 42–43 (2007) 161.
[23] L. Castoldi, I. Nova, L. Lietti, P. Forzatti, Catal. Today 96 (2004) 43.
[24] M. Colombo, I. Nova, E. Tronconi, Catal. Today 151 (2010) 223.
[25] S. Brandenberger, O. Kröcher, A. Tissler, R. Althoff, Appl. Catal. B: Environ. 95 (2010) 348.
[26] R. Kefirov, E. Ivanova, K. Hadjiivanov, S. Dzwigaj, M. Che, Catal. Lett. 125 (2008) 209.
[27] M. Ahrens, O. Marie, P. Bazin, M. Daturi, J. Catal. 271 (2010) 1.
[28] I. Nova, L. Castoldi, L. Lietti, E. Tronconi, P. Forzatti, F. Prinetto, G. Ghiotti, J. Catal. 222 (2004) 377.
[29] E. Kaiser, C. Wu, J. Phys. Chem. 81 (1977) 1701.
[30] J. Szanyi, J.H. Kwak, D.H. Kim, S.D. Burton, C.H.F. Peden, J. Phys. Chem. B 109 (2004) 27.
[31] M. Colombo, I. Nova, E. Tronconi, Appl. Catal. B: Environ. 111–112 (2012) 433.
[32] E. Millon, Ann Chimie Physique 3ème sèrie 19 (1847) 255.
[33] M. Colombo, I. Nova, E. Tronconi, Catal. Today 197 (2012) 243.
[34] L. Castoldi, L. Lietti, I. Nova, R. Matarrese, P. Forzatti, F. Vindigni, S. Morandi, F. Prinetto, G. Ghiotti, Chem. Eng. J. 161 (2010) 416.
[35] I. Malpartida, M.O. Guerrero-Pérez, M.C. Herrera, M.A. Larrubia, L.J. Alemany, Catal. Today 126 (2007) 162.
[36] I.S. Pieta, M. García-Diéguez, C. Herrera, M.A. Larrubia, L.J. Alemany, J. Catal. 270 (2010) 256.
[37] V. Matsouka, M. Konsolakis, R.M. Lambert, I.V. Yentekakis, Appl. Catal. B: Environ. 84 (2008) 715.
[38] A.A. Davydov, C.H. Rochester, Infrared Spectroscopy of Adsorbed Species on the Surface of Transition Metal Oxides, Wiley, Chichester, New York, 1990. p. 54.
[39] Y. Chi, S.S.C. Chuang, J. Phys. Chem. B 104 (2000) 4673.
[40] C. Sedlmair, K. Seshan, A. Jentys, J.A. Lercher, J. Catal. 214 (2003) 308.